Ring solitons on vortices

P. G. Kevrekidis
Program in Applied and Computational Mathematics, Princeton University, Fine Hall, Washington Road, Princeton, New Jersey 08544 and Center for Nonlinear Studies and Theoretical Division, Los Alamos National Laboratory, Los Alamos, New Mexico 87545

H. E. Nistazakis and D. J. Frantzeskakis
Department of Physics, University of Athens Panepistimiopolis, Zografos, Athens 15784, Greece

B. A. Malomed
Department of Interdisciplinary Studies, Faculty of Engineering, Tel Aviv University, Tel Aviv, Israel

A. R. Bishop
Center for Nonlinear Studies and Theoretical Division, Los Alamos National Laboratory, Los Alamos, New Mexico 87545
(Received 25 May 2001; published 20 November 2001)

Interaction of a ring dark or antidark soliton (RDS and RADS, respectively) with a vortex is considered in the defocusing nonlinear Schrödinger equation with cubic (for RDS) or saturable (for RADS) nonlinearities. By means of direct simulations, it is found that the interaction gives rise to either an almost isotropic or a spiral-like pattern. A transition between them occurs at a critical value of the RDS or RADS amplitude, the spiral pattern appearing if the amplitude exceeds the critical value. An initial ring soliton created on top of the vortex splits into a pair of rings moving inward and outward. In the subcritical case, the inbound ring reverses its polarity, bouncing from the vortex core, without conspicuous effect on the core. In the transcritical case, the bounced ring soliton suffers a spiral deformation, while the vortex changes its position and structure and also loses its axial symmetry. Through a variational-type approach to the system's Hamiltonian, we additionally find that the vortex-RDS and vortex-RADS interactions are, respectively, attractive and repulsive. Simulations with the vortex placed eccentrically with respect to the RDS or RADS reveal the generation of strongly localized multispot dark and/or antidark coherent structures. The occurrence of spiral-like patterns in many numerical experiments prompted an attempt to generate a spiral dark soliton, but the latter is found to suffer a core instability that converts it into a rotating dipole emitting waves in the outward direction.

DOI: 10.1103/PhysRevE.64.066611 PACS number(s): 05.45.Yv

I. INTRODUCTION

Ring dark solitons (RDS's) were introduced by Kivshar and Yang in Ref. [1]. Such solutions to the cubic defocusing nonlinear Schrödinger (NLS) equation in the $(2+1)$-dimensional case have attract interest because, provided that the ring's radius is small enough, they are not subject to the transverse instability characteristic of stripe (rectilinear) dark solitons. In the work [1], as well as in a subsequent one [2], it was shown how multiscale expansions can be used to derive an asymptotic equation for these small circular dips on top of a continuous-wave (cw) background. It has thus been demonstrated that, for Kerr and non-Kerr nonlinearities, small-amplitude RDS's are governed by a cylindrical Korteweg–de Vries (CKdV) equation, which was earlier known in applications to fluids and plasmas (see, e.g., Ref. [3]). In Ref. [2], it was also concluded that ring *antidark* solitons (RADS's), i.e., humps on top of the cw background rather than dips, can exist too, but only for non-Kerr (e.g., saturable) nonlinearities.

Solitary waves of the RDS type may find practical applications in the framework of the ''light-guided-by-light'' concept, due to their ability to induce built-of-light waveguides in which *multiple* weak signal beams may be guided parallel [4]. This possibility has initiated a number of experiments aimed at creating RDS's, using computer-generated holograms and other methods [5–8]. The results of these experiments were found to agree with analytical and numerical predictions [9].

Another class of fundamentally important excitations supported by NLS-type equations in $(2+1)$ dimensions are vortices, namely, topologically charged circular waves [10]. Vortices can be generated by means of appropriate computer-generated phase masks, so as to create topological phase dislocations [11,15]. The most promising application that vortices may find in photonics is also their use as controllable (moveable) effective waveguides for weak signal beams in a bulk medium [12]. Since both RDS's and RADS's, as well as vortex solitons, have become subjects of interest in experimental studies, it may be natural to consider interactions between them, i.e., the dynamics of a ring soliton located on top of a vortex, which is the subject of the present work. This may be regarded as a generalization of recent analytical and experimental studies of the interaction between stripe and vortex solitons [16].

It is relevant to mention that dynamics of ring-shaped solitons that may collapse, then bounce from the center, collapse again, and thus perform quasiperiodic pulsations in the radial direction attracted considerable attention some time ago, chiefly in the context of the two-dimensional sine-Gordon model; see, e.g., Refs. [13,14]. Unfortunately, there is virtually no real physical medium to observe numerous

effects predicted in these works, as, for instance, two-dimensional Josephson junctions cannot be uniformly driven by an external bias current. An optical field with an embedded vortex offers a unique example of a physical system where various experiments with annular solitons may be performed (although the sine-Gordon equation does not apply in this case).

However, the study of interactions of RDS's and/or RADS's with the vortex and between themselves is most relevant in the context of the above-mentioned potentially important application of the vortices as effective guides for weak optical signals. Indeed, launching a signal into the vortex (parallel to its axis) may naturally produce various perturbations that will generate one or more ring solitons, and it is then necessary to know if the vortex itself will remain really stable in the case when the amplitudes of the perturbations are finite (but, of course, not very large). We demonstrate below that this problem is quite nontrivial: despite the complete stability of the vortex against infinitesimal perturbations, the interaction of ring-shaped soliton(s), which are generated by a finite perturbation, with the vortex may give rise to a conspicuous shift of the vortex center, and break its circular symmetry, provided that the soliton's amplitude exceeds a threshold value. As well as the possibility of this, generally speaking, detrimental but nevertheless important aspect of the dynamics of ring solitons positioned on a vortex, another interesting issue may be using them as higher-order signal modes propagating in the waveguide induced by the vortex in the bulk medium. Thus, the problem of the most straightforward interest is the interaction of a RDS or RADS with the vortex core.

The interaction between a RDS or RADS and a vortex is considered in detail in the following section by means of direct simulations of the appropriate NLS model. In the case when the ring soliton's amplitude is not too small, the simulations frequently demonstrate that the soliton gives rise to spiral patterns, which suggests the question of whether a spiral generalization of the vortex may exist. This issue is considered in Sec. III, a result being that, in the self-defocusing Kerr medium, a spiral-vortex configuration is subject to a strong instability which transforms its core into a rotating dipole emitting small-amplitude waves in the outward direction. In Sec. IV we summarize the conclusions obtained in this work.

II. INTERACTIONS BETWEEN A RING DARK OR ANTIDARK SOLITON AND A VORTEX

A. The model

To study the interaction of a RDS with a vortex, we use, as a benchmark system, the $(2+1)$-dimensional defocusing NLS equation, which describes, for instance, the spatial evolution of a monochromatic transverse electromagnetic wave in a nonlinear self-defocusing medium [16]. The standard form of the NLS equation with the cubic (Kerr) nonlinearity is

$$iu_z = -(1/2)\Delta u + |u|^2 u, \tag{1}$$

where $\Delta \equiv \partial_x^2 + \partial_y^2$ is the transverse diffraction operator, and the subscript z stands for the derivative along the propagation direction. We also aim to consider equations with a more general (non-Kerr) nonlinearity of the form

$$iu_z = -(1/2)\Delta u + f(|u|^2)u, \tag{2}$$

where $f(I)$ is a positive-definite, strictly increasing monotonic function of its argument.

In accordance with the possibility suggested by the results of Ref. [2], an initial condition generating a ring soliton should be taken as a combination of the cw background u_0 and a CKdV ring solitary wave [17], which is

$$a_1(\xi,r) = -\frac{3\epsilon k}{p}\left(\frac{f_0'}{2|u_0|}\right)^{2/3}\left(\frac{r_0}{r}\right)^{2/3} \operatorname{sech}^2\phi, \tag{3}$$

$$\phi(\xi,r) \equiv \frac{1}{2}\sqrt{3k}\left(\frac{r_0}{r}\right)^{1/3} \times\left\{(2C_0)^{-2/3}\xi - \frac{3}{2}\epsilon^{3/2}kr_0\left[\left(\frac{r}{r_0}\right)^{1/3}-1\right]\right\},$$

where k is an arbitrary positive parameter of the ring soliton family, $\epsilon>0$ is a formal small parameter of the reductive multiscale expansion, $r=\sqrt{x^2+y^2}$, r_0 is the RDS radius, $\xi \equiv \epsilon^{1/2}(r-r_0)$, $C_0 \equiv f_0'|u_0|^2$, and

$$p = 3f_0' + |u_0|^2 f_0'', \tag{4}$$

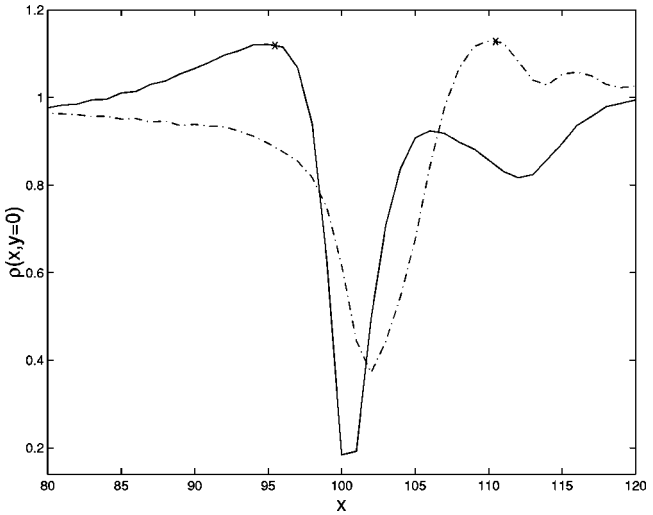

FIG. 1. Polarity reversal for a RDS bouncing from the center of the vortex. A cut of the field $\rho \equiv |u(x,y)|$ along the line $y=0$ is shown [the vortex is centered at $(x=0,y=0)$]. The solid and dash-dotted lines show the field just before the fall of the RDS onto the vortex center, and right after its bounce from the center. The position of the crest of the RDS just before and right after it collides with the vortex is marked by $\times$.

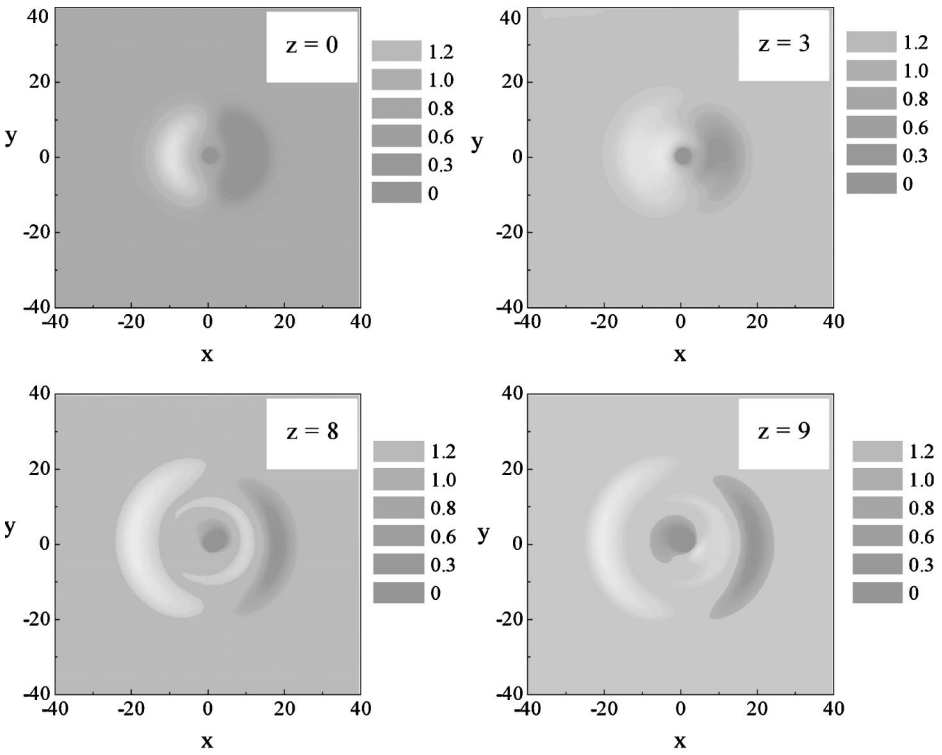

FIG. 2. The evolution of a RDS on top of the vortex in the case $\epsilon < \epsilon_{\rm cr}^{\rm dark}$ (in this case, $\epsilon = 0.1$ and $\epsilon_{\rm cr}^{\rm dark} = 0.29$). Contour plots of the absolute value of the field are shown for $z=0$, $z=3$, $z=8$, and $z=9$. It can be seen that the cylindrical symmetry of the pattern is not conspicuously broken, and no significant perturbation of the vortex core is observed.

the prime standing for the derivative of f with respect to its argument. The subscript 0 implies that the derivative is evaluated at the value of $|u|^2$ equal to the intensity $|u_0|^2 \equiv I_0$ of the cw background; hereafter, we use the normalization $I_0 = 1$.

According to Eq. (3), the excitation is dark if $p > 0$, and antidark in the opposite case. In the case of the cubic nonlinearity, $f(I) = I$, hence Eq. (4) yields $p = 3$, and the ring soliton is always dark [2]. In contrast, a saturable nonlinearity, such as

$$f(I) = \frac{I}{(1 + I/I_s)^3} \tag{5}$$

with a saturation intensity I_s, may support either dark or antidark solitons. It is easy to find that, with regard to the fact that the intensity of the cw background is normalized to be 1, it is modulationally stable if $I_s \geqslant 2$. RADS's and RDS's exist, respectively, in the cases $2 \leqslant I_s < 3$ and $I_s > 3$.

The vortex with the topological charge 1 can be created by an initial field configuration

$$u(r,\theta) = b_1(r)\exp(i\theta) \equiv \tanh(\sqrt{I_0}r)\exp(i\theta), \tag{6}$$

where r and θ are the polar coordinates in the plane (x,y). Running direct simulations of Eqs. (1) and (2) (by means of the fourth-order Runge-Kutta scheme [18] for integration in time along with a finite difference discretization in space) with free boundary conditions, we have checked that the initial conditions (6) readily give rise to a stable vortex, after some relaxation related to emission of waves in the outward radial direction. The spatial discretization step used in the simulations was typically $\Delta x \in [0.4, 0.5]$, while the runs were also performed with half the step to ensure accuracy of the results obtained. No phase instabilities were observed in either case. Typical time steps of the integrator were $\Delta t \approx 0.01$.

To study the interactions of radial solitons with the vortex, we have performed systematic simulations in which the initial conditions were taken as a superposition of the radial soliton, as given by Eq. (3), and the vortex, as given by Eq. (6). Results of the simulations are summarized below.

B. A radial dark soliton on the vortex

An initial radial perturbation corresponding to the dark waveform (3) splits into two RDS's, ingoing and outgoing ones. Similarly, an initial antidark perturbation of the same type splits into two separating RADS's. Of these, the inbound ring is of major interest, as it may strongly interact with the vortex. Next, it can be discerned in the figures shown below that, due to the slope of the vortex-field background on which the RDS or RADS is placed, the shape of the appearing ring solitons does not amount to a simple dip or hump in the radial direction, as in the previously studied case of a uniform background. Instead, the RDS appears to have a major dip accompanied by a smaller hump, and vice versa for the RADS. In fact, the RDS and RADS differ in the amplitudes of the dips and humps in their transverse ring structures.

To perform systematic simulations, we vary the amplitude of the radial-soliton component (3) in the initial conditions, fixing $k = 1$, and taking different values of ϵ. The simulations reveal that there are two different types of the behavior, depending on the size of ϵ. If ϵ is smaller than some critical value $\epsilon_{\rm dark}^{\rm (crit)}$, which, in the NLS equation with the self-

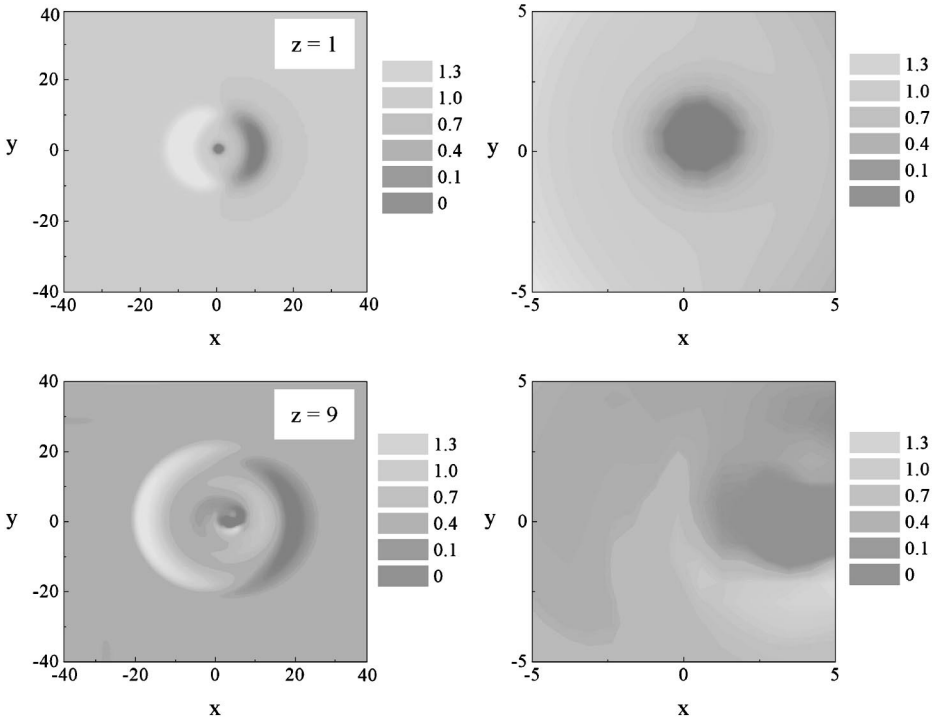

FIG. 3. The interaction between a RDS and vortex at a moderate transcritical value of the RDS amplitude, with $\epsilon=0.4$. The top panel shows the configuration shortly after the initialization, at $z=1$, when the inbound and outbound RDS's have just separated, and the vortex core is not yet affected by the RDS. The bottom left panel shows a configuration developed considerably later, at $z=9$, after the bounce of the inbound RDS from the vortex core has already occurred. The vortex shown in the bottom right panel is displaced, asymmetrically distorted, and it has energy slightly larger than that of its unperturbed counterpart, as described in the text.

defocusing cubic nonlinearity considered here, was found to be ≈ 0.29, the amplitude of the asymmetric (containing both dip and hump) inbound RDS is small, and its interaction with the vortex produces an almost isotropic pattern. In particular, after bouncing from the center of the vortex, the dip and hump parts of the RDS exchange polarities, while the vortex is not conspicuously affected. An example of such a polarity reversal is shown in Fig. 1, where comparing horizontal cuts of the absolute value of the field for the pre- and postcollision snapshots reveals the switch of the dip and hump. The interaction of the RDS with the vortex in this case is additionally demonstrated in the sequence of snapshots in Fig. 2 for $\epsilon=0.1$.

In the *transcritical case* $\epsilon>\epsilon_{\rm dark}^{(\rm crit)}$, the simulations demonstrate that the shrinking inbound RDS breaks the cylindrical symmetry of the vortex through the onset of a spiral instability. In particular, at moderate values of ϵ, as in the case shown in Fig. 3 for $\epsilon=0.4$, the dip and hump parts of the RDS are spiraling toward the vortex center, and after the interaction they eventually separate from it. At higher values of ϵ, as in the case shown in Fig. 4 for $\epsilon=0.6$, they stay attached to the center in a spiral configuration.

An important observation is that, in the present case ($\epsilon>\epsilon_{\rm dark}^{(\rm crit)}$), the size and structure of the vortex can be affected by the bounce of the RDS from its center. In particular, one can observe already from Fig. 3 that, even for moderate transcritical values of the amplitude, the vortex core gets more compressed, and its profile becomes steeper. Calculating the field energy in a box containing the vortex as

$$E_b=\int_b\left[\frac{1}{2}|\nabla u|^2+\frac{1}{2}(|u|^2-1)^2\right]$$

(where the subscript *b* has been used to denote calculation of the integral over the box), we have concluded that the interaction results in a mild increase of the energy (see Fig. 5). The energy increase becomes more substantial at larger ϵ, which is explained by a contribution of the above-mentioned spiral fragments of the RDS stuck at the vortex core.

Another important feature that can be seen in Fig. 3 is that the center of the vortex is located at different positions before and after the interaction (cf. the top right and bottom right panels of the figure), i.e., the interaction with the RDS *displaces* the center of the vortex. Additionally, it is seen that the rotational symmetry of the core is broken by the interaction. It is obvious that these effects, implying a lack of robustness of the vortices against finite disturbances, despite their well-known stability against infinitesimal perturbations, are quite important in identifying relevant parametric regions in which the vortex may be used as a conduit for (relatively) weak optical signals, as was proposed in Ref. [12].

An issue of obvious interest is whether the interaction between a RDS and the vortex core is effectively attractive or repulsive. To this end, we used the following (variational) approach. An ansatz assuming a superposition of the vortex with a RDS, the RDS radius r_0 being treated as a free parameter, was inserted into the expression for the system's Hamiltonian:

$$H=\int_0^\infty\int_0^{2\pi} r\,dr\,d\theta\left[\frac{1}{2}|\nabla u|^2+\frac{1}{2}(|u|^2-1)^2\right]. \qquad (7)$$

The resulting dependence of the potential vs r_0, obtained by numerical computation of the integral (7), is shown in Fig. 6. It is clearly seen that the interaction between the vortex core and the RDS is attractive.

We also investigated a case when the vortex was initially placed not at the center of the configuration, but rather ec-

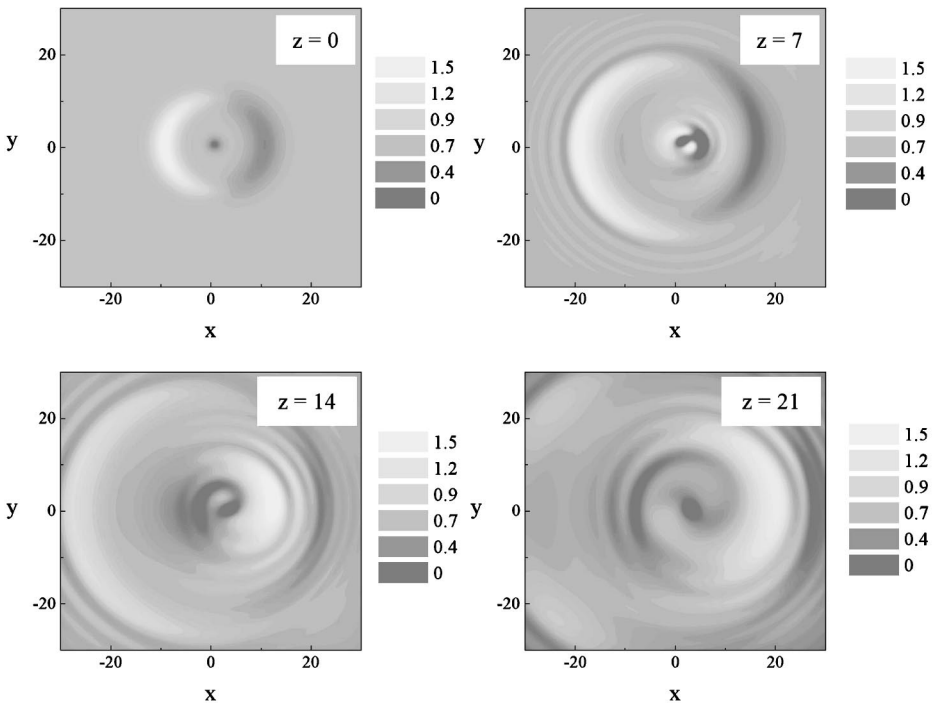

FIG. 4. The interaction of a RDS with the vortex, which generates spiral patterns at larger values of the RDS amplitude. In this case, $\epsilon=0.6$, and the panels pertain to $z=1$, $z=7$, $z=14$, and $z=21$. The spiral approach of the fragmented inbound RDS toward the vortex core can be observed. It is clearly seen that the spiral arms remain attached to the vortex core.

centrically, with respect to the RDS. In particular, we placed the vortex at different positions with respect to the RDS, following a *clock rule*: if the initial RDS is thought of as a clock frame, the vortex was placed, sequentially, at positions marked as 12:00, 1:30, 3:00, and so on. In these cases, the development of spiral patterns is, naturally, faster than in the cases with the vortex originally placed in the center of the RDS.

It is worth mentioning that effects produced by the eccentricity of a ring soliton were studied in detail in the above-mentioned two-dimensional sine-Gordon equation [14]. In that case, the result is quite different: spiral patterns do not appear; instead, the ring's eccentricity develops periodic oscillations while the soliton (quasi) periodically bounces from the center, so that the ring is sometimes compressed along the *y* axis and elongated along the *x* axis, and sometimes vice versa.

C. A radial antidark soliton on the vortex

Interaction of the RADS with the vortex in the saturable model (2),(5) resembles, in many aspects, the interaction of the RDS considered above. In particular, in this case too, a critical value $\epsilon_{\rm antidark}^{\rm (crit)}\approx 0.25$ was found, below which the interaction picture remains almost isotropic, with polarity reversal of the bouncing ring soliton and no significant changes to the vortex. For $\epsilon>\epsilon_{\rm antidark}^{\rm (crit)}$, a spiral pattern is observed and the interaction phenomenology is considerably more complicated, affecting also the position, structure, and size of the vortex. Examples of these two different types of the interaction between the RADS and the vortex are shown in Figs. 7 and 8.

However, a difference from the case of the RDS is that, in the present case, very complex interaction patterns occur if the vortex is initially placed eccentrically with respect to the RADS. An example is demonstrated in Fig. 9 for the case in which the vortex is originally placed at the position 4:30 as per the clock notation introduced above, and $\epsilon=0.4$. In particular, it can be observed that, as a result of the development

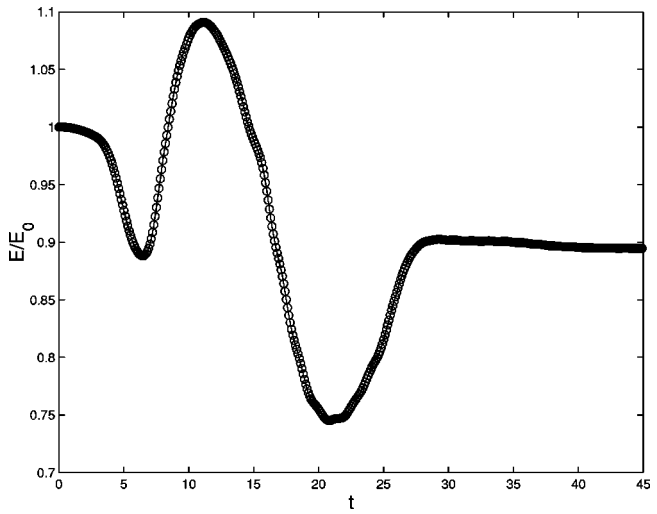

FIG. 5. The evolution of the net energy E inside a box containing the vortex (normalized to the initial energy E_0 in the same box) in the case $\epsilon=0.4$. The evolution of $E(z)$ can be explained as follows: Initially, the core emits waves, readjusting itself to an exact vortex shape, and hence its energy decreases. Subsequently, the approaching inbound RDS brings more energy, but then the interaction with it, resulting in a shift of the vortex, causes a temporary decrease of the energy. Eventually, the spiral arms detach and the former inbound RDS moves away from the box after the bounce from the vortex core, leaving the vortex (at $z\approx 28$) with an almost constant energy (it is slowly varying due to additional emission of waves), which is slightly larger than the energy that the vortex had just before the impact of the inbound RDS (at $z\approx 6$).

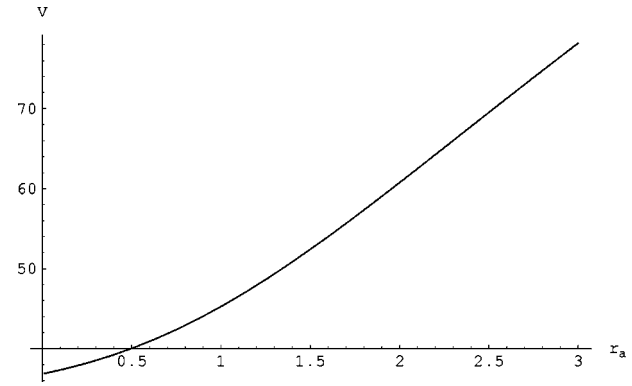

FIG. 6. The interaction potential (7) vs the radius of a RDS located on top of the vortex. It is obvious that the RDS is attracted by the vortex core. A similar picture occurs for other values of ϵ (here, $\epsilon=0.1$).

of a spiral pattern in the shrinking inbound RADS, the antidark portion of the RADS gets fragmented into very localized coherent structures, and the vortex is no longer present in the final configuration, having transferred its vorticity to the spiral dip fragments in the final configuration.

We also calculated the Hamiltonian

$$H=\int_0^{\infty}\int_0^{2\pi} r dr d\theta\left(|\nabla u|^2+\frac{1}{2}I_s^3\frac{I_s+2|u|^2}{I_s+|u|^2}\right) \tag{8}$$

for the RADS-vortex configuration, in order to estimate the sign of the corresponding interaction [cf. Eq. (7)]. The result is that, unlike the effective potential shown in Fig. 6, the potential generated by the Hamiltonian (8) is a monotonically decreasing function of r_0; hence the vortex core tends to *repel* the antidark ring.

III. SPIRAL DARK SOLITONS

The presence of spiral arms in many of the figures displayed above, as well as in Fig. 2 of Ref. [16], suggests the question whether stable spiral dark or antidark solitons may exist. To address the issue, we generated initial conditions that consisted of spiral arms emanating from the vortex core on top of the uniform background; see the top left panel of Fig. 9. Such initial configurations were constructed by replacing $r\rightarrow r+S\theta$, with an integer "spin" S, in the numerically found expression for the zero-vorticity RDS (so that the net "spin" of the perturbation, taking into regard the vorticity of the underlying vortex, is $S+1$). Then the configuration was allowed to evolve, governed by the $(2+1)$-dimensional NLS equation (1) with the defocusing Kerr nonlinearity. An example of the evolution is displayed in Fig. 10.

The following persistent features were observed in all the numerical experiments with the spiral solitons: an instability appears at the core of the spiral, which enforces generation of a dipolelike structure rotating around the center and emitting waves outward (so that the structure resembles a sprinkler). Upon collision with the domain boundaries, the emitted waves give rise to interference patterns which can be clearly discerned in Fig. 10. It should be noted, however, that these numerical experiments were performed for spiral dark solitons with different numbers of spiral arms and the instability converting the core into a dipole was observed *in all the cases studied*. It should also be mentioned, for the simulation of Fig. 10, that the phenomena occurring near the core

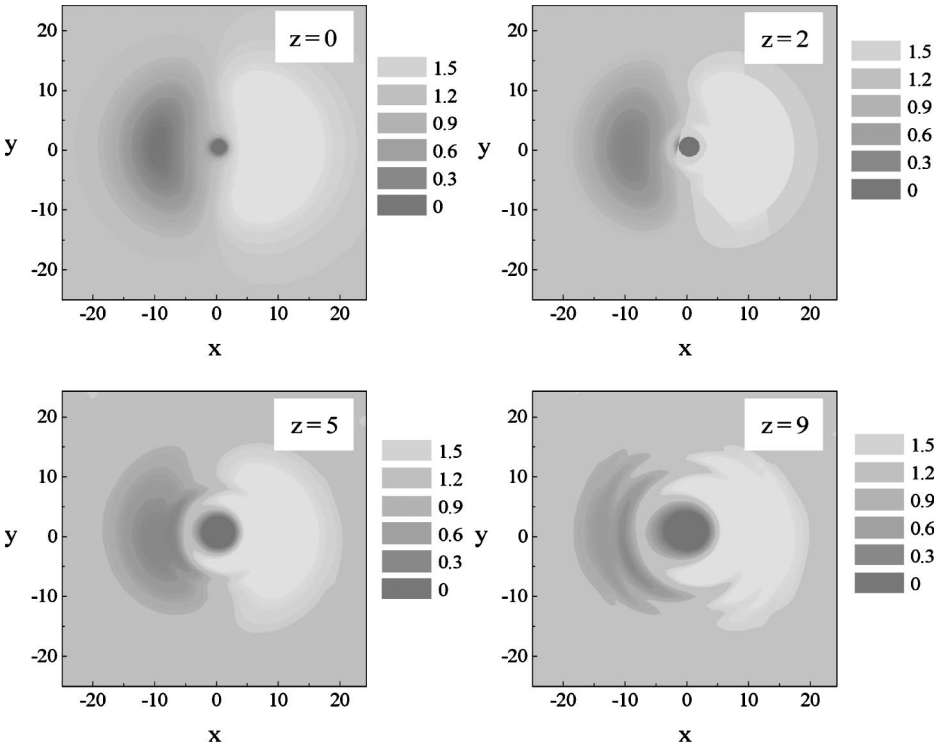

FIG. 7. Evolution of the absolute value of the field in the case of the interaction of a RADS with the vortex in the subcritical case, with $\epsilon=0.1$. The panels shown pertain to $z=0$, $z=2$, $z=5$, and $z=9$.

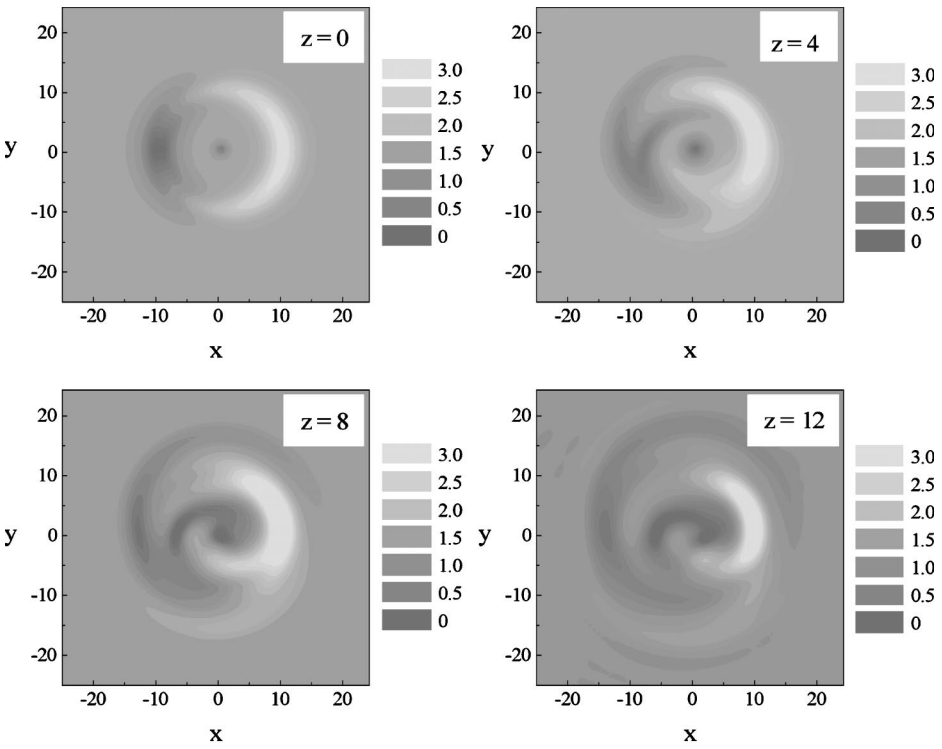

FIG. 8. The same as in Fig. 7, but for the transcritical case, with $\epsilon = 0.6$. The panels shown pertain to $z = 0$, $z = 4$, $z = 8$, and $z = 12$.

are well screened from the domain boundary by the spiral arms and hence were *not* affected for the duration of the numerical experiment (in which the instability developed—in fact, already at the second snapshot of Fig. 10) by the presence of the boundary.

Thus, it can be concluded that, although spiral arm fragments appear to propagate as stable configurations, the core instability of the spiral dark solitary wave transforms its central part into a wave-emitting dipole. The fact that a dipole is a more stable configuration is not surprising in view of recent results for focusing media [19], where such patterns were observed to be stable in a wide parametric range. It

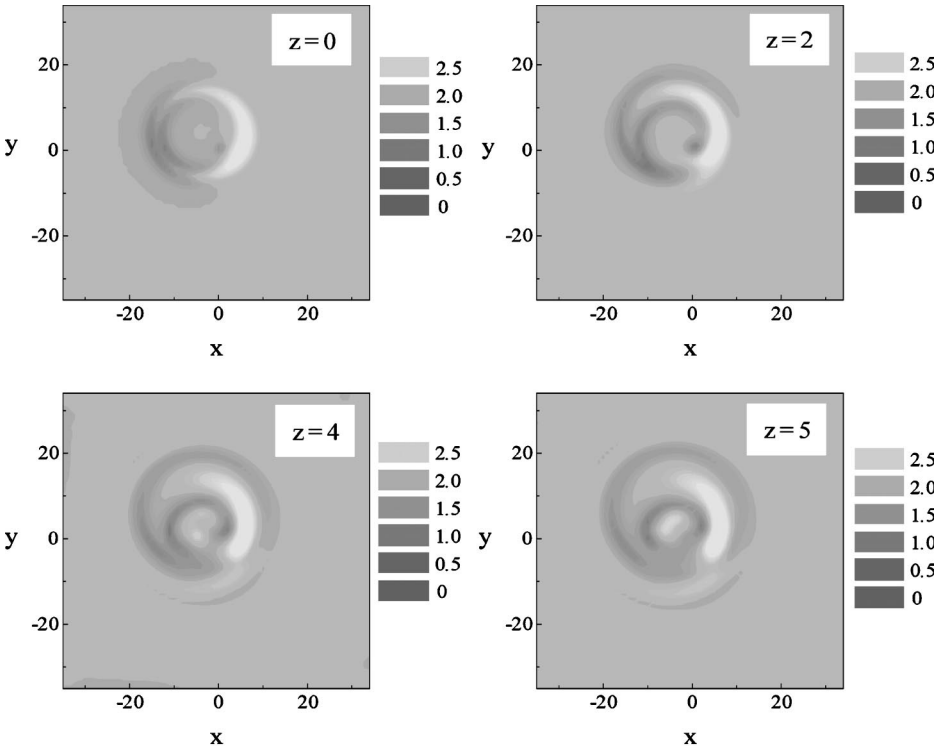

FIG. 9. The eccentric vortex initially placed at the position 4:30 inside the RADS, in terms of the clock rule. In this case, $\epsilon = 0.4$, and the panels shown pertain to $z = 0$, $z = 2$, $z = 4$, and $z = 5$.

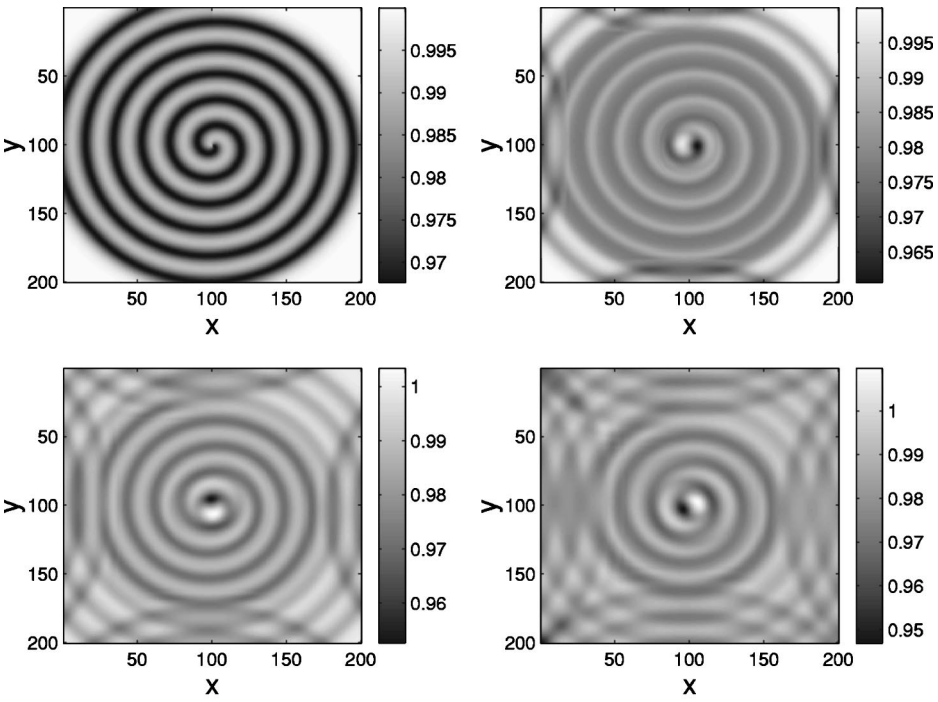

FIG. 10. The evolution of a configuration that was constructed on purpose as a spiral dark soliton. The top left panel shows the initial configuration proper, and the subsequent top right, bottom left, and bottom right panels show results in $\Delta z = 4$ steps. It can be seen that the outer portions of the spiral move outward, creating interference patterns due to their interaction with the boundary. Simultaneously, the core very rapidly converts itself into a dipole rotating around its center, emitting additional waves outward.

should be noted, however, that in the latter case such configurations were stationary (nonrotating).

IV. CONCLUSION

In this work, interactions between dark and antidark annular solitary waves with a vortex were examined in the framework of the $(2+1)$-dimensional NLS equation with both Kerr and non-Kerr (saturable) defocusing nonlinearities. It was found that the interactions produce very different results, depending on the amplitude of the (anti)dark-soliton component in the initial configuration. If the amplitude is smaller than a certain critical value, the ring soliton bounces from the vortex core with polarity reversal, without significantly affecting the vortex. On the other hand, if the amplitude exceeds the critical value, the RDS and RADS are subject to an instability that breaks their isotropy and lends them a spiral shape. In that case, the interaction with the RDS or RADS affects the vortex, changing its location, size, and intrinsic structure. Evaluating the potential of the interaction between the ring soliton and vortex, we have concluded that the interaction is attractive and repulsive for the dark and antidark solitons, respectively. It was also shown that eccentricity in the initial position of the vortex's core relative to the ring soliton can give rise to an even richer interaction phenomenology including the possibility of fragmentation of the RADS and transformation of the original vortex into a set of spiral dips that inherit its vorticity.

The observation of spiral-shaped objects in many simulations reported in this work, as well as in previous work, suggested a search for possible spiral dark solitons. As a result, we have found that, even though curved armlike structures can exist and propagate apparently stably in a self-defocusing Kerr medium, the core of the corresponding spiral dark soliton is always subject to an instability that transforms it into a rotating dipole sprinkling spiral waves in the outward direction.

The observation of strong localization events in some cases (such as in the case of the interaction of a RADS with an eccentric vortex) suggests the question of whether such objects as *antidark vortices* may exist. Even though the answer was negative in the present case, the search for entities of this type in models with cubic-quintic or saturable nonlinearities may produce positive results.

Very recently, a paper [20] appeared that extends the findings of Ref. [16] to the interaction of plane waves and nonlinear stripe dark solitary waves with vortices. In Ref. [20], it was found (as we also confirmed and quantified herein for the interaction of the vortex with RDS's and RADS's) that spiral arms develop as a result of the interaction, and that the vortex is displaced upon its interaction with the dark solitary wave [see Fig. 3(c) in Ref. [20]]. In that work, the interaction was interpreted as a classical (linear or nonlinear) version of the Aharonov-Bohm effect.

ACKNOWLEDGMENTS

Research at the Los Alamos National Laboratory is conducted under the auspices of the U.S. Department of Energy under Contract No.W-7405-ENG-36. B.A.M. appreciates support from the Binational (U.S.-Israel) Science Foundation through Grant No. 1999459, and partial support from the European Research and Development Office of the U.S. Air Force within the framework of the Window-on-Science Program.

[1] Yu.S. Kivshar and X. Yang, Phys. Rev. E **50**, R40 (1994).
[2] D.J. Frantzeskakis and B.A. Malomed, Phys. Lett. A **264**, 179 (1999).
[3] E. Infeld and G. Rowlands, *Nonlinear Waves, Solitons and Chaos* (Cambridge University Press, Cambridge, 1990).
[4] A. Dreischuh, V. Kamenov, and S. Dinev, Appl. Phys. B: Lasers Opt. **63**, 145 (1996).
[5] S. Balushev *et al.*, Phys. Rev. E **52**, 5517 (1995).
[6] A. Dreischuh *et al.*, Appl. Phys. B: Lasers Opt. **62**, 139 (1996).
[7] D. Neshev *et al.*, Appl. Phys. B: Lasers Opt. **64**, 429 (1997).
[8] W.H. Lee, Prog. Opt. **16**, 119 (1978).
[9] A. Dreischuh *et al.*, e-print nonlin.PS/0006044.
[10] G.A. Swartzlander, D.R. Andersen, J.J. Regan, H. Yin, and A. Kaplan, Phys. Rev. Lett. **66**, 1583 (1991).
[11] J. Christou, V. Tikhonenko, Yu.S. Kivshar, and B. Luther-Davies, Opt. Lett. **21**, 1649 (1996).
[12] A.H. Calrsson *et al.*, Opt. Lett. **25**, 660 (2000).
[13] J. Geicke, Phys. Scr. **29**, 431 (1984); E.M. Maslov, Physica D **15**, 433 (1985); B.A. Malomed, *ibid.* **24**, 155 (1987).
[14] P.L. Christiansen, N. Grønbech-Jensen, P.S. Lomdahl, and B.A. Malomed, Phys. Scr. **55**, 131 (1997).
[15] D.V. Petrov *et al.*, Opt. Lett. **23**, 1444 (1998).
[16] Yu.S. Kivshar *et al.*, Opt. Lett. **25**, 123 (2000); D. V. Petrov, Opt. Quantum Electron (to be published).
[17] R.S. Johnson, Wave Motion **30**, 1 (1999).
[18] E. Hairer, S. P. Nørsett, and G. Wanner, *Solving Ordinary Differential Equations I: Nonstiff Problems* (Springer-Verlag, Berlin, 1993).
[19] J.J. Garcia-Ripoll, V.M. Perez-Garcia, E.A. Ostrovskaya, and Yu.S. Kivshar, Phys. Rev. Lett. **85**, 82 (2000); W. Krolikowski *et al.*, *ibid.* **85**, 1424 (2000), and references therein.
[20] D. Neshev, A. Nepomnyashchy, and Yu.S. Kivshar, Phys. Rev. Lett. **87**, 043901 (2001).